Molecular Design of Near-Infrared Fluorescent Pdots for Tumor Targeting: Aggregation-Induced Emission versus Anti-Aggregation-Caused Quenching

*Wei-Kai Tsai,[a†] Chun-I Wang,[b†] Chia-Hsien Liao,[a] Chun-Nien Yao,[b] Tsai-Jhen Kuo,[a] Ming-Ho Liu,[a] Chao-Ping Hsu,[c] Shu-Yi Lin,[b] Chang-Yi Wu,[d] Joseph R. Pyle,[e] Jixin Chen,[e] and Yang-Hsiang Chan[f]**

[a]*Department of Chemistry, National Sun Yat-sen University, 70 Lien Hai Road, Kaohsiung, Taiwan 80424.*

[b]*Institute of Biomedical Engineering and Nanomedicine, National Health Research Institutes, 35 Keyan Road, Zhunan, Taiwan 35053.*

[c]*Institute of Chemistry, Academia Sinica, Taipei, Taiwan 115.*

[d]*Department of Biological Sciences, National Sun Yat-sen University, 70 Lien Hai Road, Kaohsiung, Taiwan 80424*

[e]*Department of Chemistry & Biochemistry, Ohio University, Athens, Ohio 45701, United States*

[f]*Department of Applied Chemistry, National Chiao Tung University, Hsinchu, Taiwan 30050*

[†]*Both authors contributed equally to this work*

E-mail: yhchan@mail.nsysu.edu.tw

Supplementary Information

Materials. The chemicals used in the experiments were purchased from Alfa Aesar, Sigma-Aldrich, TCI, and Acros. All chemicals were used as received unless unless specified otherwise. All ^{1}HNMR spectra were obtained on a Bruker AV300 spectrometer (300 MHz). PS-PEG-COOH (M_n~365,000) was purchased from Polymer Source, Inc., while PF-TFQ-BODIPY (M_n~14000), TFQ, and BODIPY was synthesized according to our previously published work.[1] TPE and Pttc derivatives were synthesized according to previously published reports[2-6] and thus only simplified synthetic procedures were described herein. Other compounds were synthesized with modified procedures and the appropriate literatures were cited for each compounds. All water used is deionized (18.2 MΩ•cm). The calculated inter-fragment torsional potentials of the donor-acceptor and the donor-bridge are included in Figure S1. The potentials are then fitted in the Ryckaert-Bellemans function: $U = \sum_{n=0}^{5} C_n[\cos(\phi - 180°)]^n$, with fitted parameters listed in Table S1. We note that there is no inter-fragment torsional potential of Pttc-BODIPY and Pttc-TFQ because they are linked by a linear triple bond. All the force field parameters and the corresponding atom coordinates are included in the additional supporting data files "PF-TFQ-BODIPY.top", "TPE-TFQ-BODIPY.top", "Pttc-TFQ-BODIPY.top", "PF-BODIPY-PF.gro", "PF-TFQ-PF-TFQ.gro", "TPE- BODIPY-TPE.gro", "TPE-TFQ-TPE-TFQ.gro", "PTTC- BODIPY-PTTC.gro" and "PTTC-TFQ-PTTC-TFQ.gro".

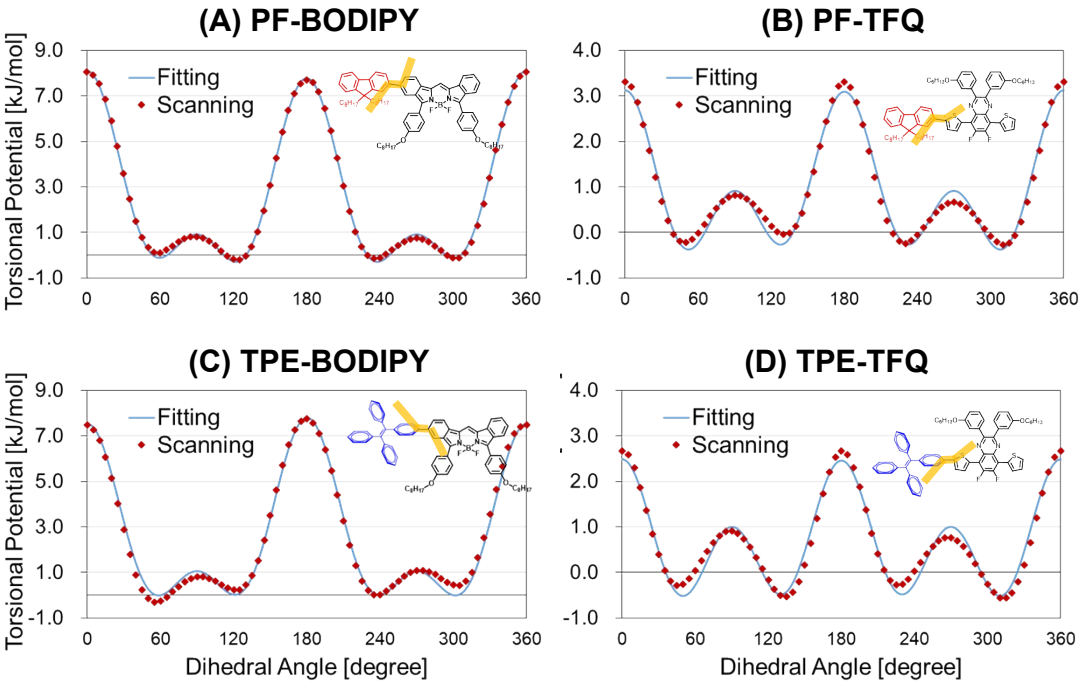

Figure S1. Torsional potentials obtained with the PM6 semi-empirical Hamiltonian (red dot) and the numerical fitting (blue line). The corresponding torsional angles scanned are depicted in the insets, which are (A) PF-BODIPY, (B) PF-TFQ, (C) TPE-BODIPY, and (D) TPE-TFQ, respectively.

Table S1. Parmeters for the Torsional potentials.

(kJ/mol)	PF-BODIPY	PF-TFQ	TPE-BODIPY	TPE -TFQ
C_0	0.9146	0.91356	1.0583	1.00179
C_1	-0.02472	0.07193	-0.02337	0.05906
C_2	-8.25152	-6.57926	-7.77622	-7.22409
C_3	-0.67928	0.12255	0.20953	-0.08535
C_4	15.2751	8.77387	14.3838	8.69392
C_5	0.54026	-0.20960	-0.05649	0.01209

Synthesis of (E)-1,2-bis(4-bromophenyl)-1,2-diphenylethene, ***1****.*[2-3] Compound **1** was synthesized through Mcmurry reaction. Briefly, Zn powder (3.8g, 58.1 mmol) was added into a three-neck round-bottom flask under nitrogen atmosphere. 70 mL of freshly distilled THF was added for stirring at room temperature and then titanium (IV) chloride (3.3 mL, 29.9 mmol) was added at 0 °C. The mixture was heated to 80 °C and stirred for

2.5 h. After that, 4-bromobenzophenone (1.5g, 5.74 mmol) was added dropwise at 0 °C and then heated to 80 °C to react for another 40 h. After the reaction, the mixture was cooled down and the solvent was removed by rotary evaporator. The residue was dissolved in CH_2Cl_2 and then extracted with brine. After the extraction, CH_2Cl_2 was separated and dried over magnesium sulfate and then CH_2Cl_2 was removed by rotary evaporator. The crude product was further purified on a silica-gel column with hexane as eluent to yield 760 mg (54 %) of compound **1** as a white solid. ^{1}H NMR (300 MHz, $CDCl_3$): δ = 7.26-7.20 (m, 4H), 7.15-7.09 (m, 6H), 7.01-6.96 (m, 4H), 6.90-6.85 (m, 4H).

Synthesis of (E)-1,2-diphenyl-1,2-bis(4-(4,4,5,5-tetramethyl-1,3,2-dioxaborolan-2-yl)phenyl)ethene, ***TPE****.*[2-3] To a flask was added 500 mg (1.02 mmol) of compound **1**, 518 mg (2.0 mmol) of bis(pinacolato)diboron, and 600 mg (6.12 mmol) of potassium acetate in 20 mL of DMF under nitrogen atmosphere, and 37 mg (0.05 mmol) of Pd(dppf)Cl_2 was added into the flask in one portion. After that, the reaction mixture was heated to 110 °C for 36 h and then cooled down to room temperature. The obtained residue was dissolved in CH_2Cl_2 to extract with brine. The CH_2Cl_2 layer was separated and dried by magnesium sulfate. Then CH_2Cl_2 was removed by rotary evaporator. The crude product was further purified on a silica-gel column with hexane/ethylene acetate (4:1, v/v) as eluent to yield 180 mg (30 %) of **TPE** as a yellow solid. The obtained product contains both E/Z isomers and were not specially separated. ^{1}H NMR (300 MHz, $CDCl_3$): δ = 7.52 (d, J = 9.0 Hz, 4H), 7.09-7.01 (m, 14H), 1.32 (s, 24H).

Synthesis of (5s,14s)-5,7,12,14-tetrahydro-5,14:7,12-bis([1,2]benzeno)pentacene-6,13-dione, ***2****.*[4-5] To a single-neck round-bottom flask was added 2 g (18.5 mmol) of p-benzoquinone, 4.95 g (27.8 mmol) of anthracene, and 30 mL of mesitylene. The reaction

mixture was heated to 165 °C to reflux for 48 h and then cooled down to room temperature. The precipitated residue was washed by hexane for 2-3 times. The solid was then dissolved in glacial acetic acid completely and 0.77 g (4.61 mmol) of potassium bromate in water was added slowly to obtain yellow precipitation. The crude product was further purified on a silica-gel column with hexane/CH_2Cl_2 (1:1, v/v) as eluent to yield 2.23 g (43 %) of compound **2** as a yellow solid. ^{1}H NMR (300 MHz, $CDCl_3$): δ = 7.37-7.34 (m, 8H), 6.98-6.96 (m, 8H), 5.75 (s, 4H).

*Synthesis of Compound **3**.*[4-5] To a single-neck round-bottom flask was added 469 mg (1.0 mmol) of compound **2** under nitrogen atmosphere and 15 mL of freshly distilled THF was added at 0 °C. To another single-neck round-bottom flask was added 0.35 mL (2.5 mmol) of (trimethylsilyl)acetylene and 15 mL of freshly distilled THF under nitrogen atmosphere, and then 2.5 mmol of *n*-butyllithium was added at 0 °C. The two solutions were stirred at 0 °C for 1 h and then the one containing *n*-butyllithium was transferred into another one very slowly via a syringe needle. After that, the mixture was allowed to worm up to room temperature and kept stirring for 8 h. The reaction was cooled to 0 °C again and 1 mL of 10% HCl was added slowly to terminate the reaction. The residue was dissolved in CH_2Cl_2 and then extracted with brine. After the extraction, CH_2Cl_2 was separated and dried over magnesium sulfate and then CH_2Cl_2 was removed by rotary evaporator. The crude product was further purified by washing with acetone to yield 530 mg (81 %) of compound **3** as a white solid. ^{1}H NMR (300 MHz, $CDCl_3$): δ = 7.35-7.28 (m, 8H), 6.93-6.90 (m, 8H), 5.50 (s, 4H), 0.19 (s, 18H).

*Synthesis of (5s,14s)-6,13-diethynyl-5,7,12,14-tetrahydro-5,14:7,12-bis([1,2]benzene)pentacene, **Pttc**.*[2-3] 530 mg (0.81 mmol) of compound **3** in 10 mL of

acetone was added into a round-bottomed flask under nitrogen atmosphere and then 510 mg (2.25 mmol) of tin (II) chloride in 50% 10 mL of acetic acid was added slowly into the flask. The mixture was stirred for 24 h at room temperature. After the reaction, the precipitates were dissolved in CH_2Cl_2 and extracted with $NaHCO_3$. The organic layer was then separated and dried over magnesium sulfate. CH_2Cl_2 was further removed by rotary evaporator to obtain the crude product. The crude product was further purified by washing with hexane and acetone to afford 298 mg (59 %) of compound **4** as a white solid. ^{1}H NMR (300 MHz, $CDCl_3$): δ = 7.32-7.31 (m, 8H), 6.95-6.92 (m, 8H), 5.77 (s, 4H), 0.50 (s, 18H). Compound **Pttc** was obtained quantitatively by stirring a mixture solution containing 300 mg (0.48 mmol) of compound **4**, 5 mL of THF, 5 mL of MeOH, and 1 mL of 30% KOH for 5 h at room temperature. The precipitates were collected and then dissolved in CH_2Cl_2 to extract with brine. The organic layer was then separated and dried over magnesium sulfate. CH_2Cl_2 was further removed by rotary evaporator to afford compound **Pttc** as a white solid. ^{1}H NMR (300 MHz, $CDCl_3$): δ = 7.37-7.34 (m, 8H), 6.96-6.93 (m, 8H), 5.82 (s, 4H), 3.70 (s, 2H).

General Procedures of Polymerization. Compound PF-TFQ-BODIPY and TPE-TFQ-BODIPY were synthesized according to our previously reported works.[1, 7-8] For the synthesis of PF-TFQ-BODIPY and TPE-TFQ-BODIPY, we employed Suzuki−Miyaura coupling as displayed in Scheme 1. For Pttc-TFQ-BODIPY, the Sonogashira polycondensation reaction was utilized for polymerization.[9] Briefly, monomer 5 or TPE or Pttc (0.5 mmol), monomer TFQ (0.48 mmol), and monomer BODIPY (0.02 mmol) were used in the polymerization crossing-coupling. After the polymerization, the products were purified by reprecipitation in CH_2Cl_2/methanol and washed with cold

acetone to obtain 50-80 mg of polymers. PF-TFQ-BODIPY: M_n 12970, M_w 15453, PDI 1.19; TPE-TFQ-BODIPY: M_n 17060, M_w 22934, PDI 1.34; Pttc-TFQ-BODIPY: M_n 12887, M_w 22908, PDI 1.78.

Synthesis of Monomer TFQ. The detailed synthesis of monomer TFQ was reported by our previously published work[8] with synthetic steps as summarized below.

Scheme S1. Synthetic routes of monomer TFQ.[1]

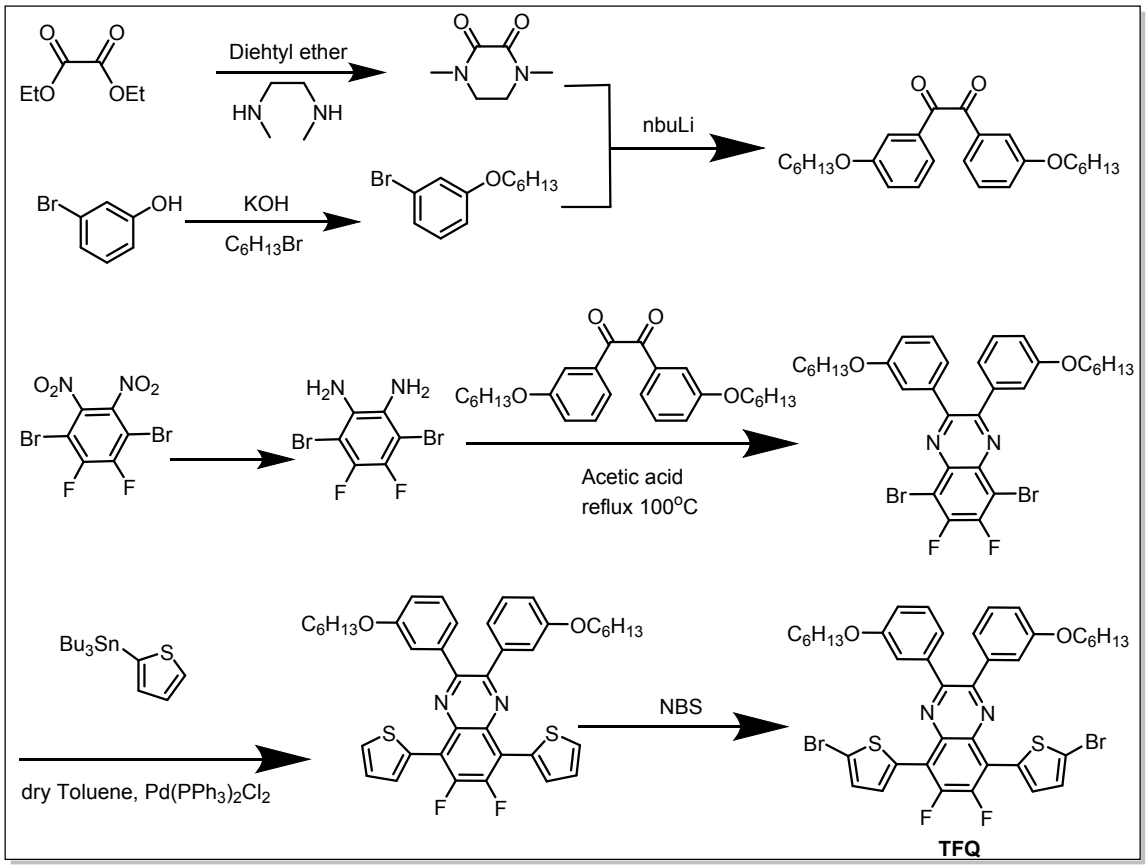

Preparation of Pdots. Typically, 200 μL of semiconducting polymer PF-TFQ-BODIPY or TPE-TFQ-BODIPY or Pttc-TFQ-BODIPY solution (1 mg/mL in THF), 20 μL of PS-PEG-COOH (1 mg/mL in THF) were mixed well in 5 mL THF. The THF solutions containing polymers were injected into 10 mL H_2O under vigorous sonication. After that, THF was gradually removed by purging nitrogen gas on a 90 °C hotplate for

60 min. The Pdot solutions were further filtered by a 0.2 μm polyethersulfone syringe filter to get rid of possible large aggregates during Pdot preparation.

Bioconjugation and Characterization of Pdots. Bioconjugation was performed by using the EDC-catalyzed reaction between carboxylate-functionalized Pdots and amine-containing streptavidin. In a typical bioconjugation reaction, 80 μL of polyethylene glycol (5% w/v PEG, MW 3350) and 80 μL of concentrated HEPES buffer (1 M) were added to 4 mL of Pdot solution, resulting in a Pdot solution in 20 mM HEPES buffer with a pH ~7.4. Then 240 μL of streptavidin (1 mg/mL) was added to the solution and mixed well by stirring. After that, 80 μL of freshly-prepared EDC solution (5 mg/mL in MilliQ water) was added to the solution, and the mixture was stirred for 4 hours at room temperature. After bionconjugation, 80 μL of BSA (10 wt%) was added to the Pdot solution and the reaction was continued for another 20 minutes. A 80-μL aliquot of Triton X-100 in MilliQ water (2.5 wt%) was added to the Pdot-streptavidin mixture. The mixture was then transferred to a centrifugal ultrafiltration tube (Amicon® Ultra-4, MWCO: 100kDa), and then concentrated to 0.5 mL by centrifugation. Finally, the Pdot-streptavidin bioconjugates were purified by gel filtration using Sephacryl HR-300 gel media. To conjugate Pdots with folate-PEG-NH_2,[1] 120 μL of Folate-PEG-NH_2 (1 mg/mL) in DMSO and 80 μL of freshly-prepared EDC solution (5 mg/mL in MilliQ water) was added to a 4mL of Pdot solution. The mixture was stirred for 4 h and then worked up using the same protocol as mentioned above. The folate-modified Pdots (FA-Pdots) were then used for in vivo tumor imaging in mice.

The average particle size was determined by dynamic light scattering and transmission electron microscopy (TEM). TEM images of the synthesized Pdots were acquired using a JEOL 2100 transmission electron microscope at an acceleration voltage of 200 kV. For TEM, a drop of Pdot aqueous solution was placed onto a carbon-coated grid and allowed to evaporate at room temperature. The absorption spectra of Pdots were measured using UV-visible spectroscopy (Dynamica Halo DB20S, Dynamica Scientific). The fluorescence spectra were collected using a Hitachi F-7000 fluorometer (Hitachi, Tokyo, Japan) under 450 nm excitation. Absolute fluorescence quantum yield of Pdots was determined by using an integrating sphere unit of Hitachi F-7000 fluorescence spectrophotometer.

Single-Particle Brightness Measurements. For single-particle brightness experiments, we spread diluted Pdot or Qdot705 solutions on piranha-cleaned glass coverslips and dried under vacuum. The samples were imaged with a Nikon inverted microscope equipped an Andor iXon Ultra 897 camera under epifluorescence mode. A 473 nm laser beam with a power 1 mW was used to direct into the inverted microscope. For measuring each frame, a 100X oil immersed objective (NA = 1.49), 100 EM gain, and 0.02 s exposure time were employed. At least five movies were recorded for individual samples at different locations. The intensity distribution included all frames, and therefore contained the photobleaching ones.

Flow Cytometry. Flow cytometry measurements were performed on freshly Pdot-labeled MCF-7 cells (~10^5 cells/0.3 mL). The cells were analyzed by a Moxi GO II (ORFLO, Ketchum, ID) equipped with a 488 nm laser and a 561 nm long-pass filter. The data were processed with FlowJo software.

Cell Culture and Labeling. The breast cancer cell line MCF-7 was ordered from Food Industry Research and Development Institute (Taiwan). Primary cultured HeLa cells were grown in Dulbecco's Modified Eagle Medium (cat. no. 11885, Invitrogen) supplemented with 10% fetal bovine serum (FBS) and 1% penicillin-streptomycin solution (5000 units/mL penicillin G, 50 μg/mL streptomycin sulfate in 0.85% NaCl) at 37 °C with 5% CO_2 humidified atmosphere. MCF-7 cells were cultured at 37 °C, 5% CO_2 in RPMI 1640 medium supplemented with 10% FBS and 1% penicillin-streptomycin solution. The cells were pre-cultured in a T-25 flask and allowed to grow for 5-7 days prior to experiments until ~80% confluence was reached. To prepare cell suspensions, the adherent cancer cells were quickly rinsed with media and then incubated in 0.8 mL of trypsin-ethylenediaminetetraacetic (EDTA) solution (0.25 w/v % trypsin, 0.25 g/L EDTA) at 37 °C for 3 min. The cell suspension solution was then centrifuged at 1000 rpm for 5 min to precipitate the cells to the bottom of the tube. After taking out the upper media, the cells were rinsed and resuspended in 5 mL of culture media. Approximately tens of thousands cells were split onto a glass-bottomed culture dish and allowed to grow for 12 h before Pdot labeling. Prior to fluorescence imaging, the cells were rinsed with PBS buffer to remove any nonspecifically bound Pdots on the cell surface.

For cell labeling experiments, BlockAid™ blocking buffer was purchased from Invitrogen (Eugene, OR, USA). For labeling cell-surface markers with IgG, a million MCF-7 cells in 100-μL labeling buffer (1× PBS, 2 mM EDTA, 1% BSA) was incubated with 0.3 μL of 0.5 mg/mL primary biotin anti-human CD326 EpCAM antibody (BioLegend, San Diego, CA, USA) on a rotary shaker in the dark and at room temperature for 30 minutes, followed by a washing step using labeling buffer. Then the

cells were incubated with 1.5 nM Pdot-streptavidin conjugates in BlockAid™ buffer for 30 min on a shaker in the dark and at room temperature, followed by two washing steps with labeling buffer. Prior to cell incubation, Pdot solutions were sonicated for 3 min in order to disperse any potential aggregates. Negative controls were obtained by incubating cells with Pdot-streptavidin conjugates in the absence of primary biotinylated-antibody. Cell fixation was performed by dissolving the cell pellet obtained by centrifugation in 500 μL of fixing buffer (1× PBS, 2 mM EDTA, 1% BSA, 1% PFA).

Cell Imaging. The fluorescence spectra of Pdot-tagged cells were acquired with a fluorescence confocal microscope (Zeiss LSM 700) under ambient conditions (24 ± 2 ^{o}C). The confocal fluorescence images were collected using a diode laser at 533 nm (~15 mW) as the excitation source and an integration time of 1.6 μs/pixel. A Carl Zeiss 63x ("C-Apochromat" 63x/1.2 W Corr) objective was utilized for imaging and spectral data acquisition; the laser was focused to a spot size of ~7 μm^2. The blue fluorescence was collected by filtering through a 450/35 band-pass (λ_{ex} = 405 nm) while the red fluorescence was collected by filtering through a 650 long-pass (λ_{ex} = 533 nm).

MTT Assay. The cellular cytotoxicity of the Pdots was examined on HeLa cells. The number of viable cells was determined using the MTT assay with 3-(4,5-dimethylthiazole-2-yl)-2,5-phenyltetrazolium bromide. HeLa cells were first seeded in each well of a 24-well culture plate and then incubated with various concentrations of Pdots (500 pM, 1 nM, and 2 nM) for 6 h, 12 h, and 24 h. After that, 20 μL (5 mg/mL) of MTT aqueous solution was added to each well and the cells were further incubated for 4 h at 37 °C to deoxidize MTT. The medium was then washed out and 300 μL of DMSO was added into each well to dissolve formazam crystals. Absorbance was measured by a

BioTek ELx800 microplate reader at 570 nm, while the cells cultured with the pure medium (e.g., without Pdots) served as controls.

In vivo imaging on zebrafish. The transgenic zebrafish, *Tg(kdrl:eGFP)*^{la116} expressing eGFP in the endothelial cells, were maintained at 28 °C and bred under standard conditions with approval from National Sun Yat-sen University Animal Care Committee. For angiography imaging, 37 nL Pdots (125 nM) in 20 mM HEPES buffer was injected into the sinus venosus of the anaesthetized zebrafish embryos 3 day post fertilization (dpf) with 5% (v/v) tricaine (Sigma). The injected embryos were recovered for 30 minutes, immobilized in 1.5% low melting point agarose (invitrogen), and then imaged immediately using a fluorescence confocal microscope (Nikon D-Eclipse C1). The green fluorescence was collected by filtering through a 515/30 band-pass (λ_{ex} = 488 nm) while the red fluorescence was collected by filtering through a 570 long-pass (λ_{ex} = 488 nm).

In Vivo Tumor Targeting in Mice. Animal procedures were approved by the Institutional Animal Care and Use Committee (IACUC) of NHRI. Seven-week-old female BALB/c nude mice were purchased from National Laboratory Animal Center, and housed under specific pathogen-free conditions. The facility was maintained at 24 °C with a 12 h light/12 h dark cycle. To establish tumors in Seven-week-old female BALB/c nude mice, 2 million SKOV3 cells suspended in 100ul of 50 v/v% mixture of matrigel in supplemented RPMI1640 were injected subcutaneously in the flank of the mice. Tumors were grown until a single aspect was ~7 mm (approximately 30 days) before used for NIR imaging. The nude mice were randomly allocated to two groups for different formulations. For one were injected with Pdots (200 μl, 2 nM) via intravenous injection;

Another one were injected with folate-modified Pdots (200 μl, 2 nM) through the tail vein. *In vivo* fluorescence tumor imaging was performed and analyzed using a Xenogen apparatus (IVIS Imaging Systems, Caliper Life Sciences) by using 500 nm laser excitation (30 nm bandwidth) equipped with a 720 nm emission band-pass filter (20 nm bandwidth). The radiance e□ciency (p/s/cm2/sr) was used for quantitative region of interest analysis.

Simulation Methodology. In this work, we investigated two model systems for Pdots with MD simulation: (1) the oligomer systems consist of 2500 donor-bridge-donor-bridge (DBDB) tetramers and 50 donor-acceptor-donor (DAD) model trimers (with system size ~ 260 × 120 × 130 $Å^3$), and (2) the monomer system where donor, bridge and acceptor units are separated, where 490 donor, 490 bridge and 49 acceptor molecules are simulated (with the system size approximately equals to 130 × 70 × 90 $Å^3$). The evaluation of force field for the MD simulation and simulation details are as described below.

Force Field. For conjugated polymers, there exist a few sets of force field describing the intramolecular and intermolecular interactions in the MD simulation, especially for describing thermal-annealing condensed systems.[10-14] Considering the transferability to include different monomer units in a copolymer, the OPLS (Optimized Potentials for Liquid Simulations)[15-17] seems ideal for this purpose.[18] However, due to the extended π-conjugation along the polymer backbone, the original OPLS force field is unable to accurately capture conformational and structural properties, and therefore further adjustments of torsional potentials and atomic partial charges are necessary.[10-14, 19-20] We followed the recommended procedure described in the literature[11] to construct the torsional potentials of the donor-bridge and donor-acceptor linkage. The torsional potentials were calculated with the corresponding angles scanned from 0° to 360° with

steps of 5°. For each calculation, we constrained the dihedral angle between each unit and perform geometry optimization on all remaining degree of freedom, and the calculation was performed with PM6 semi-empirical Hamiltonian.[21] The resulting torsional potential energy surfaces were fitted with the Ryckaert-Bellemans function: $U = \sum_{n=0}^{5} C_n[\cos(\phi - 180°)]^n$. On the other hand, atomic partial charges were calculated from each individual (donor, bridge and acceptor) unit using the "Charges from the Electrostatic Potential on a Grid" (CHELP) method at the B3LYP /6-31+G** level. All quantum-chemical calculations are performed using the Gaussian 09 program package.[22] With regarding to the force field parameters of individual units, we followed the improved OPLS-based force field reported for PF, TFQ, and TPE,73-75. The force field of Pttc and BODIPY are taken from common OPLS parameters.

Simulation Details. Previously, there are literatures demonstrating a rational strategy for a thermal-annealing condensed system that produces a realistic ensemble of conjugated-polymer chain conformations.[23-25] Following a similar strategy, we started with a low-density arrangement for both the oligomer and monomer systems. The DAD oligomers (or the acceptor monomers) are uniformly mixed with the DBDB oligomers (the donor and bridge monomers, for the monomer system) to avoid artificial aggregation structure. The system was first equilibrated using *NPT* ensemble at 600 K and 100 bar for a duration of 2 ns, followed by annealing from 600 K to 300 K in a linear and continuous fashion within 1 ns (which corresponds to an annealed rate of 300 K ns^{-1}). Then, each simulation system is carried out at 1 bar and 300 K for 5 ns to help relax the changes due to the pressure adjustment. The trajectory data gathered from the final 5 ns are utilized for subsequent analyses. The MD simulation was performed using the GROMACS package

(version 2016.4)[26] with GPU acceleration (NVIDIA Tesla P100). The equations of motion were integrated using the velocity Verlet algorithm with a time step of 2 fs. All simulations were conducted at a target system pressure and various target system temperatures by using Berendsen *NPT* ensemble, with a coupling constant of 0.5 ps for both thermostat and barostat. Periodic boundary conditions in all three directions were implemented. Long-range electrostatic interactions are treated using the smoothed-particle-mesh-Ewald (SPME) technique, with a precision of 10^{-5} and a real space cutoff of 15 Å. The same cutoff distance is used for the truncation of Lennard-Jones interactions, where standard geometric combining rules are adopted for any unlike pair of atoms.

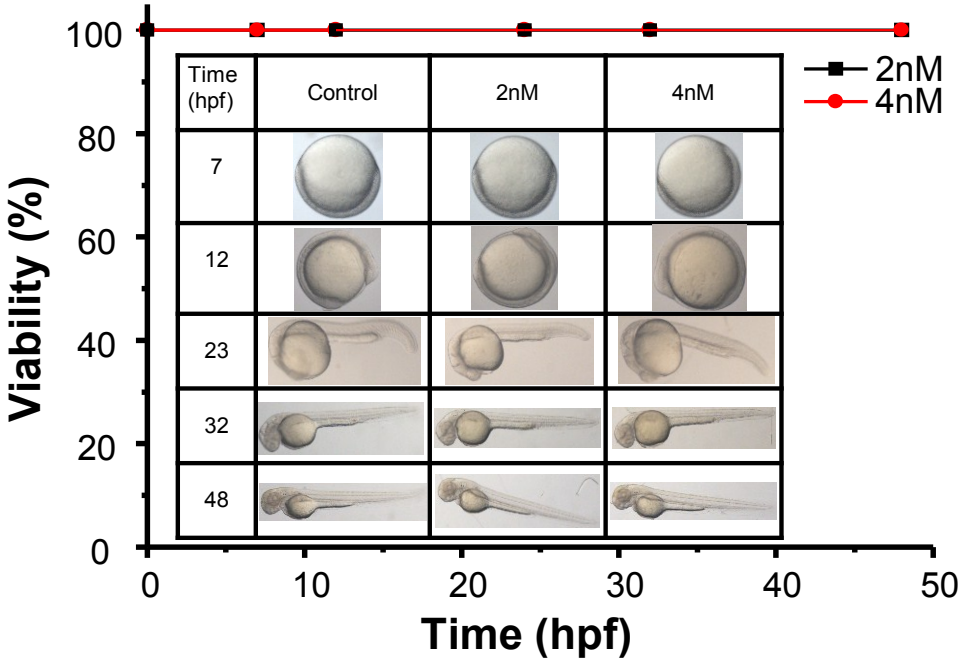

Figure S2. Biotoxicity assessment of Pdots by the zebrafish model. Time course recording morphology of zebrafish embryos exposed to 2 and 4 nM Pdot solutions in the period of 0−48 h postfertilization (hpf).

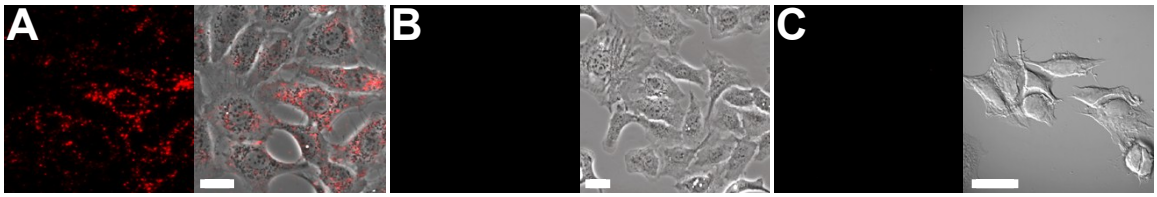

Figure S3. (A) Confocal fluorescence microscopy images of folate-receptor positive cells (SKOV-3 cells) labeled by Pdot-folate conjugates. The red emission in the left panel was attributed to Pdot-folate conjugates. The right panel displays the fluorescence image overlaid with the bright-field image. (B) Images of negative control samples where SKOV-3 cells were incubated with bare Pdots. (C) Images of negative control samples where folate-receptor negative cells (MCF-7 cells) were incubated with Pdot-folate conjugates. The scale bars are 50 μm.

We also performed the experiment of hepatotoxicity by intravenously injecting PBS buffer (control) and Pdot-folate conjugates into two separate mice. After 24 h post-injection, we measured the values of AST (aspartate aminotransferase; GOT, glutamate oxalacetate transaminase) and ALT (alanine aminotransferase; GPT, glutamate pyruvate transaminase) in serum to evaluate the liver function under Pdot treatment. Serum levels of AST at 24 h after injection were measured to be 119 and 75 U/L for PBS-treated and Pdot-treated mice, respectively. For the serum levels of ALT at 24 h after injection, they were determined to be 39 and 32 U/L for PBS-treated and Pdot-treated mice, respectively. Both values are in the normal ranges for PBS-treated or Pdot-treated mouse, indicating that the livers are still in normal function for both mice. We further carried out histological examination of livers by analyzing the H&E staining of liver tissues for both mice (Figure S4). The results suggest that Pdots have negligible hepatotoxicity.

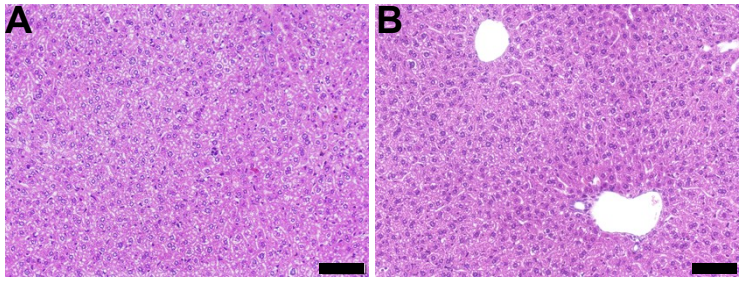

Figure S4. H&E staining of liver sections from (A) PBS-treat mouse and (B) Pdot-treated mouse at 24 h post-injection. The scale bars are 50 μm.

^{1}H NMR of **compound 1**

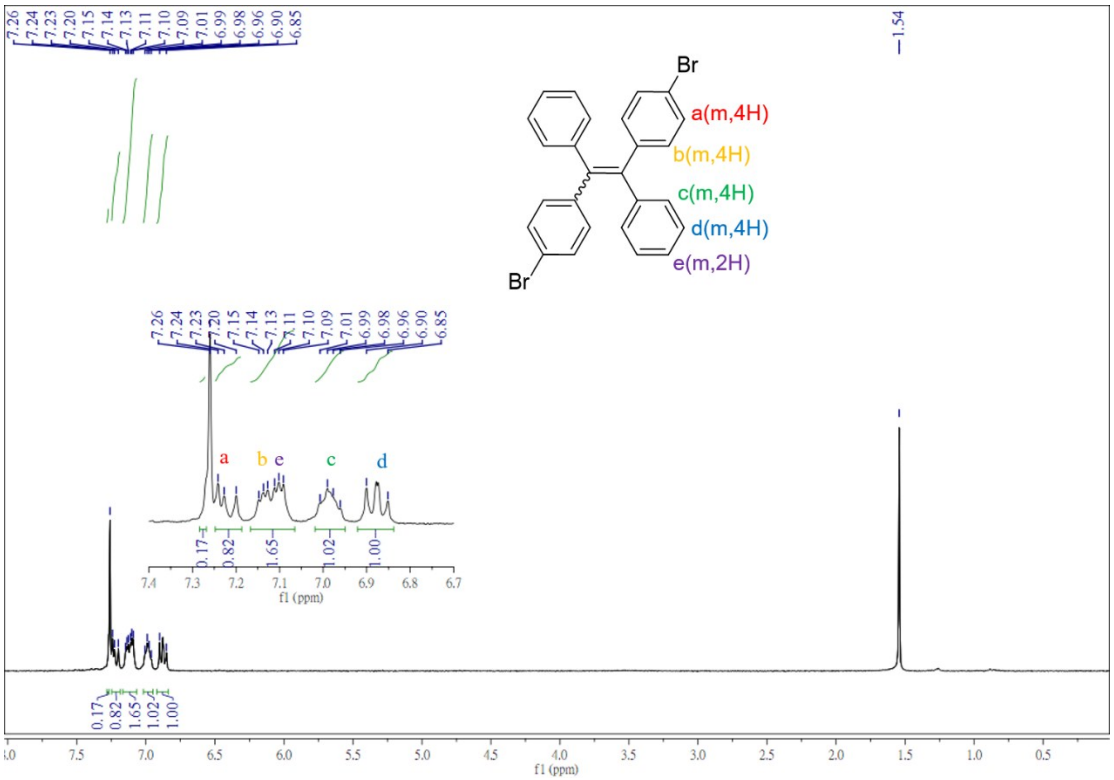

^{1}H NMR of **compound TPE**

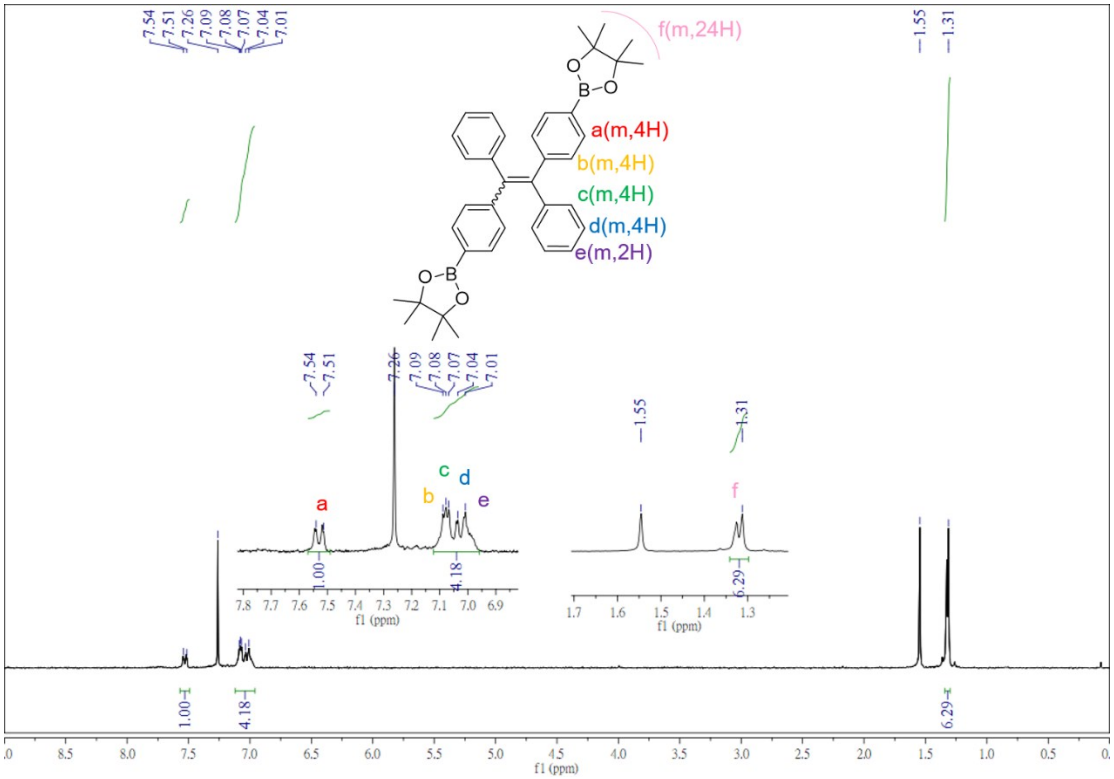

^{1}H NMR of **compound 2**

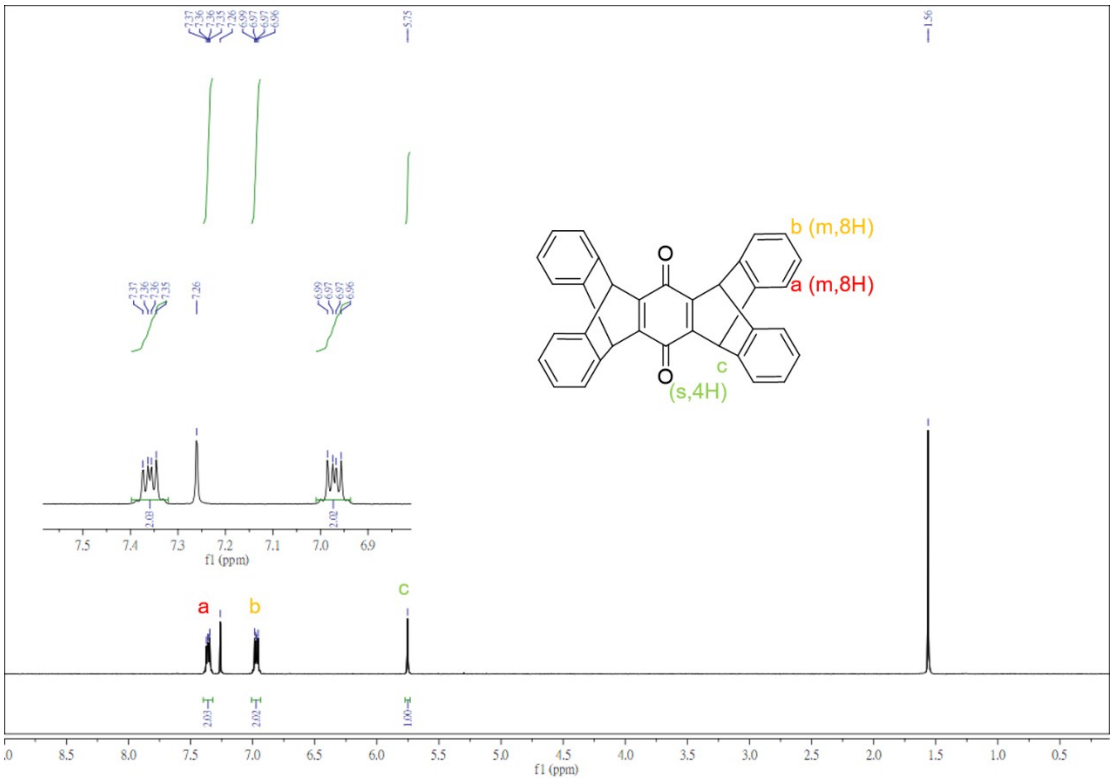

^{1}H NMR of **compound 3**

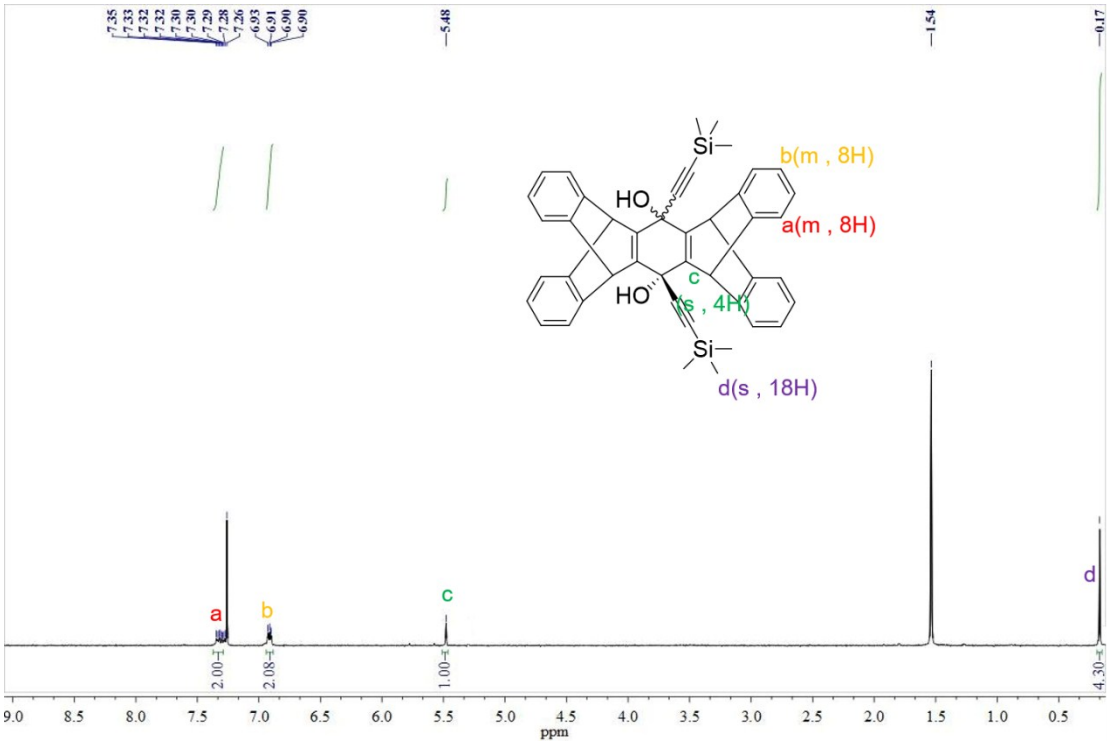

^{1}H NMR of **compound 4**

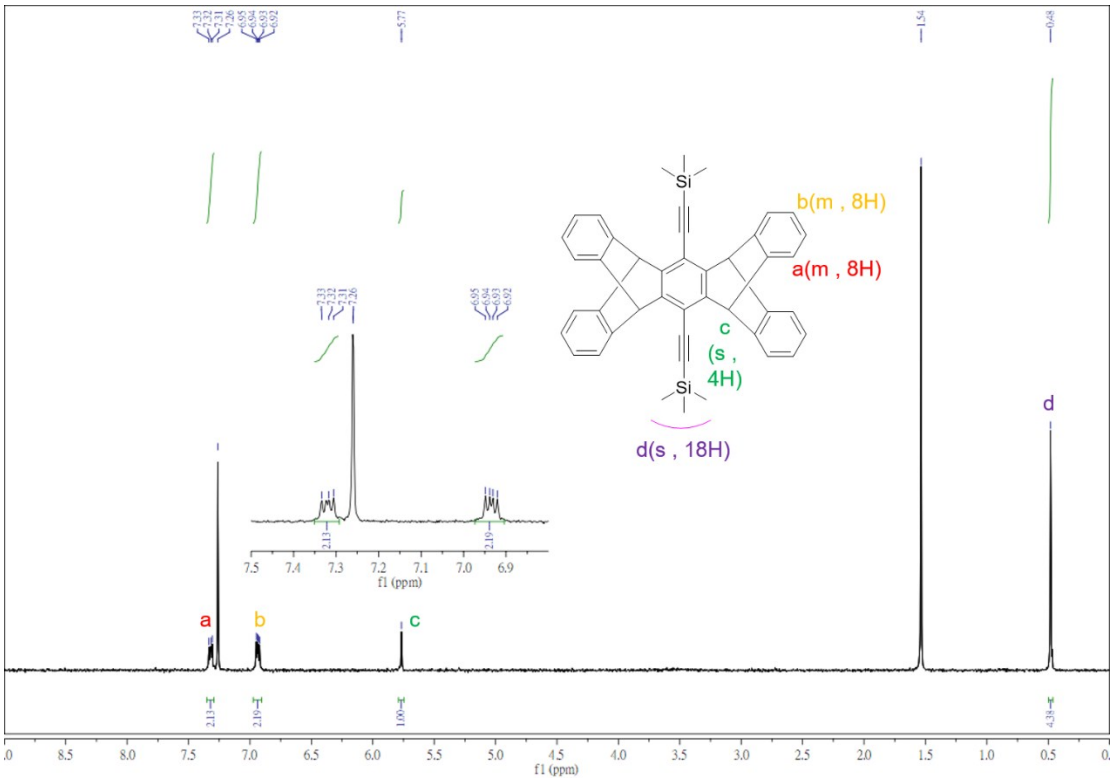

^{1}H NMR of **compound Pttc**

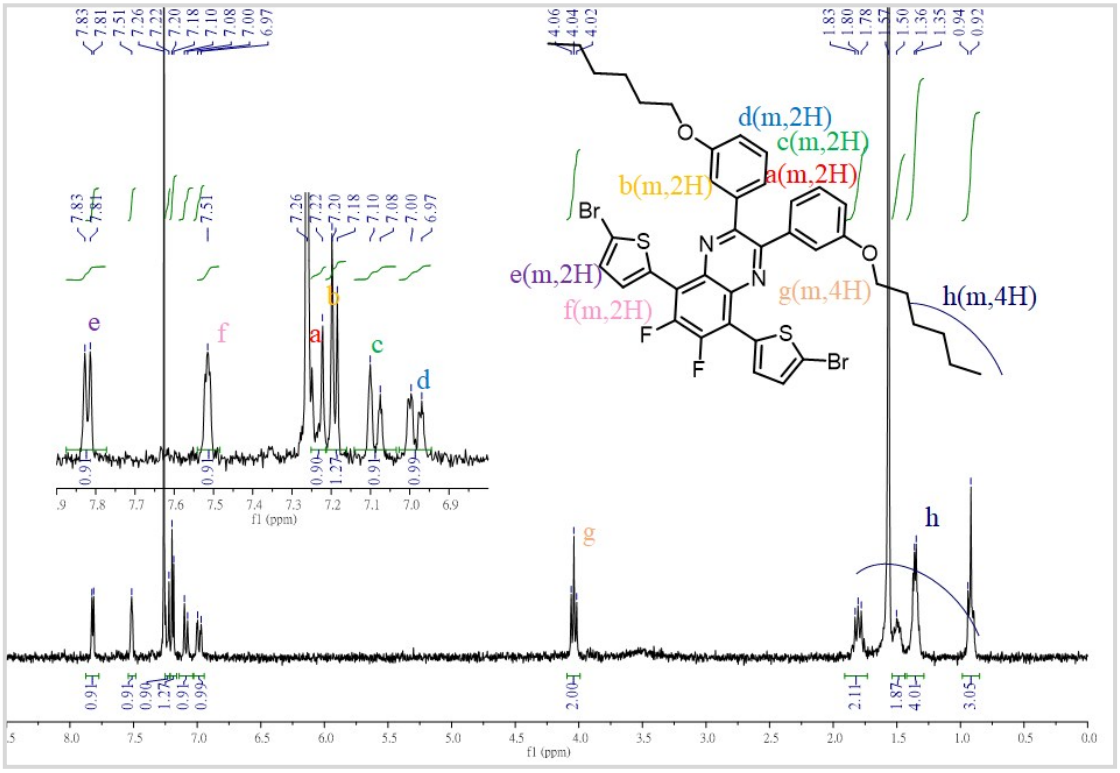
d(m,2H)
c(m,2H)
a(m,2H)
b(m,2H)
e(m,2H)
f(m,2H)
g(m,4H)
h(m,4H)
f1 (ppm)

^{1}H NMR of **compound TFQ**

1. Ke, C.-S.; Fang, C.-C.; Yan, J.-Y.; Tseng, P.-J.; Pyle, J. R.; Chen, C.-P.; Lin, S.-Y.; Chen, J.; Zhang, X.; Chan, Y.-H., Molecular Engineering and Design of Semiconducting Polymer Dots with Narrow-Band, Near-Infrared Emission for in Vivo Biological Imaging. *ACS Nano* **2017**, *11*, 3166-3177.
2. Wang, J.; Mei, J.; Yuan, W.; Lu, P.; Qin, A.; Sun, J.; Ma, Y.; Tang, B. Z., Hyperbranched Polytriazoles with High Molecular Compressibility: Aggregation-Induced Emission and Superamplified Explosive Detection. *J. Mater. Chem.* **2011**, *21*, 4056-4059.
3. Bai, W.; Wang, Z.; Tong, J.; Mei, J.; Qin, A.; Sun, J. Z.; Tang, B. Z., A Self-Assembly Induced Emission System Constructed by the Host-Guest Interaction of AIE-Active Building Blocks. *Chem. Commun.* **2015**, *51*, 1089-1091.
4. Yang, J.-S.; Swager, T. M., Fluorescent Porous Polymer Films as TNT Chemosensors: Electronic and Structural Effects. *J. Am. Chem. Soc.* **1998**, *120*, 11864-11873.
5. Bouffard, J.; Swager, T. M., Fluorescent Conjugated Polymers That Incorporate Substituted 2,1,3-Benzooxadiazole and 2,1,3-Benzothiadiazole Units. *Macromolecules* **2008**, *41*, 5559-5562.
6. Ghosh, K. R.; Saha, S. K.; Gao, J. P.; Wang, Z. Y., Direct Detection of Ultralow Trace Amounts of Isocyanates in Air Using a Fluorescent Conjugated Polymer. *Chem. Commun.* **2014**, *50*, 716-718.
7. Chen, C.-P.; Huang, Y.-C.; Liou, S.-Y.; Wu, P.-J.; Kuo, S.-Y.; Chan, Y.-H., Near-Infrared Fluorescent Semiconducting Polymer Dots with High Brightness and Pronounced Effect of Positioning Alkyl Chains on the Comonomers. *ACS Appl. Mater. Interfaces* **2014**, *6*, 21585-21595.
8. Liu, H.-Y.; Wu, P.-J.; Kuo, S.-Y.; Chen, C.-P.; Chang, E.-H.; Wu, C.-Y.; Chan, Y.-H., Quinoxaline-Based Polymer Dots with Ultrabright Red to Near-Infrared Fluorescence for In Vivo Biological Imaging. *J. Am. Chem. Soc.* **2015**, *137*, 10420-10429.
9. Popere, B. C.; Pelle, A. M. D.; Poe, A.; Balaji, G.; Thayumanavan, S., Predictably Tuning the Frontier Molecular Orbital Energy Levels of Panchromatic Low Band Gap BODIPY-Based Conjugated Polymers. *Chem. Sci.* **2012**, *3*, 3093-3102.
10. DuBay, K. H.; Hall, M. L.; Hughes, T. F.; Wu, C.; Reichman, D. R.; Friesner, R. A., Accurate Force Field Development for Modeling Conjugated Polymers. *J. Chem. Theory Comput.* **2012**, *8*, 4556-4569.
11. Jackson, N. E.; Kohlstedt, K. L.; Savoie, B. M.; Olvera de la Cruz, M.; Schatz, G. C.; Chen, L. X.; Ratner, M. A., Conformational Order in Aggregates of Conjugated Polymers. *J. Am. Chem. Soc.* **2015**, *137*, 6254-6262.
12. Vehoff, T.; Kirkpatrick, J.; Kremer, K.; Andrienko, D., Atomistic force field and electronic properties of carbazole: from monomer to macrocycle. *Phys. Stat. Sol. (b)* **2008**, *245*, 839-843.
13. Moreno, M.; Casalegno, M.; Raos, G.; Meille, S. V.; Po, R., Molecular Modeling of Crystalline Alkylthiophene Oligomers and Polymers. *J. Phys. Chem. B* **2010**, *114*, 1591-1602.

14. Bhatta, R. S.; Yimer, Y. Y.; Perry, D. S.; Tsige, M., Improved Force Field for Molecular Modeling of Poly(3-hexylthiophene). *J. Phys. Chem. B* **2013**, *117*, 10035-10045.
15. Jorgensen, W. L.; Maxwell, D. S.; Tirado-Rives, J., Development and Testing of the OPLS All-Atom Force Field on Conformational Energetics and Properties of Organic Liquids. *J. Am. Chem. Soc.* **1996**, *118*, 11225-11236.
16. Jorgensen William, L.; Laird Ellen, R.; Nguyen Toan, B.; Tirado-Rives, J., Monte Carlo simulations of pure liquid substituted benzenes with OPLS potential functions. *J. Comput. Chem.* **1993**, *14*, 206-215.
17. Jorgensen, W. L.; Schyman, P., Treatment of Halogen Bonding in the OPLS-AA Force Field: Application to Potent Anti-HIV Agents. *J. Chem. Theory Comput.* **2012**, *8*, 3895-3901.
18. Do, K.; Ravva, M. K.; Wang, T.; Brédas, J.-L., Computational Methodologies for Developing Structure–Morphology–Performance Relationships in Organic Solar Cells: A Protocol Review. *Chem. Mater.* **2017**, *29*, 346-354.
19. Bloom, J. W. G.; Wheeler, S. E., Benchmark Torsional Potentials of Building Blocks for Conjugated Materials: Bifuran, Bithiophene, and Biselenophene. *J. Chem. Theory Comput.* **2014**, *10*, 3647-3655.
20. Wildman, J.; Repiščák, P.; Paterson, M. J.; Galbraith, I., General Force-Field Parametrization Scheme for Molecular Dynamics Simulations of Conjugated Materials in Solution. *J. Chem. Theory Comput.* **2016**, *12*, 3813-3824.
21. Stewart, J. J. P., Optimization of parameters for semiempirical methods V: Modification of NDDO approximations and application to 70 elements. *J. Mol. Model.* **2007**, *13*, 1173-1213.
22. Frisch, M. J.; Trucks, G. W.; Schlegel, H. B.; Scuseria, G. E.; Robb, M. A.; Cheeseman, J. R.; Scalmani, G.; Barone, V.; Mennucci, B.; Petersson, G. A.; Nakatsuji, H.; Caricato, M.; Li, X.; Hratchian, H. P.; Izmaylov, A. F.; Bloino, J.; Zheng, G.; Sonnenberg, J. L.; Hada, M.; Ehara, M.; Toyota, K.; Fukuda, R.; Hasegawa, J.; Ishida, M.; Nakajima, T.; Honda, Y.; Kitao, O.; Nakai, H.; Vreven, T.; Montgomery, J. A.; Peralta, J. E.; Ogliaro, F.; Bearpark, M.; Heyd, J. J.; Brothers, E.; Kudin, K. N.; Staroverov, V. N.; Kobayashi, R.; Normand, J.; Raghavachari, K.; Rendell, A.; Burant, J. C.; Iyengar, S. S.; Tomasi, J.; Cossi, M.; Rega, N.; Millam, J. M.; Klene, M.; Knox, J. E.; Cross, J. B.; Bakken, V.; Adamo, C.; Jaramillo, J.; Gomperts, R.; Stratmann, R. E.; Yazyev, O.; Austin, A. J.; Cammi, R.; Pomelli, C.; Ochterski, J. W.; Martin, R. L.; Morokuma, K.; Zakrzewski, V. G.; Voth, G. A.; Salvador, P.; Dannenberg, J. J.; Dapprich, S.; Daniels, A. D.; Farkas; Foresman, J. B.; Ortiz, J. V.; Cioslowski, J.; Fox, D. J., Gaussian 09, Revision A.02. Wallingford CT, **2009**.
23. Wang, C. I.; Hsu, C. H.; Hua, C. C., The correspondence between the conformational and chromophoric properties of amorphous conjugated polymers in mesoscale condensed systems. *Phys. Chem. Chem. Phys.* **2017**, *19*, 20818-20828.
24. Qin, T.; Troisi, A., Relation between Structure and Electronic Properties of Amorphous MEH-PPV Polymers. *J. Am. Chem. Soc.* 2013, *135* (30), 11247-11256.
25. Ma, H.; Qin, T.; Troisi, A., Electronic Excited States in Amorphous MEH-PPV Polymers from Large-Scale First Principles Calculations. *J. Chem. Theory Comput.* **2014**, *10*, 1272-1282.

26. Abraham, M. J.; Murtola, T.; Schulz, R.; Páll, S.; Smith, J. C.; Hess, B.; Lindahl, E., GROMACS: High performance molecular simulations through multi-level parallelism from laptops to supercomputers. *SoftwareX* **2015**, *1-2*, 19-25.